

# Investigation of photonic spin texture in valley photonic crystals

Hironobu Yoshimi<sup>1</sup> and Hibiki Kagami<sup>2</sup>

<sup>1</sup>Iwamoto lab., Graduate School of Engineering, The University of Tokyo

<sup>2</sup>Nishiyama lab., Graduate School of Engineering, Tokyo Institute of Technology

## Author introduction

Hironobu Yoshimi

Engaged in research on integrated photonic devices based on topological valley photonic crystals. In this research, he was responsible for the design and fabrication of valley photonic crystals, and the measurement and analysis of photonic band structures.

Hibiki Kagami

Engaged in research on integrated photonic devices using photonic topological insulators. In this research, he was responsible for the measurement and analysis of photonic band structures.

## Abstract

We observed photonic band structure of valley photonic crystals (VPhCs) and worked on the experimental observation of topological spin texture of light called meron and anti-meron. Si slab VPhCs are designed and a structure with Dirac type dispersion relation above the light line is found. The structure is fabricated and polarization-resolved band structure measurements are performed using a photonic band structure microscope. As a result, we found a polarization distribution that is suggestive of meron and antimeron spin texture.

## Background

Topological photonics is a rapidly advancing field that combines the knowledge of photonics and topology, and is expected to pioneer new photonic control technologies and their applications [1]. Among them, innovative optical control technologies such as unidirectional light propagation [2], optical waveguides with suppressed bending loss [3], and unidirectional laser oscillation [4] are particularly attractive in various fields, including photonic integrated circuits.

While the above phenomena are mainly focused on band topology in momentum space,

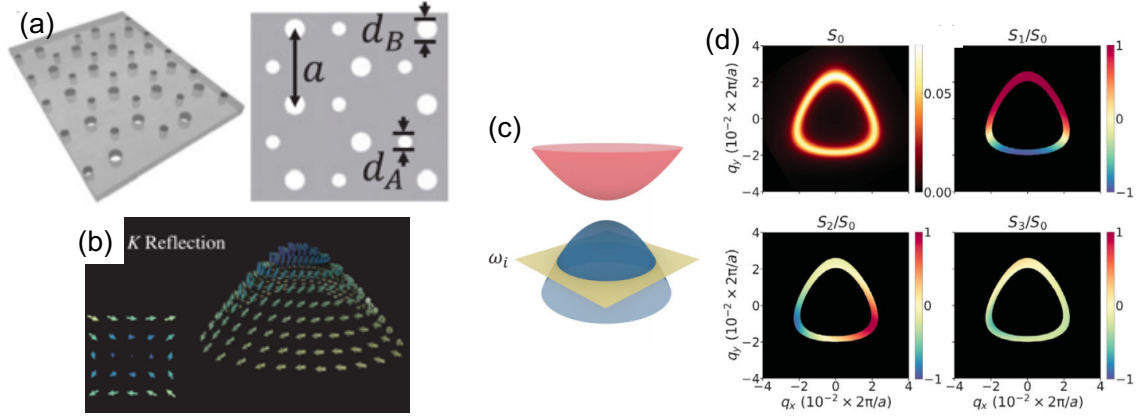


Fig. 1 Meron spin textures proposed in the previous study. (a) Target VPhC slab. (b) Antimeron around the valley of the K point. (c) Schematic of the calculation of the polarization state for each frequency in the band. (d) Polarization distribution in the isofrequency plane. [9]

optical phenomena focused on topology in real space have also attracted attention. Optical vortices and vector beams with topological charge in the polarization distribution in real space are expected to have applications in optical tweezers [5], optical communications [6], and laser processing [7]. In addition, light with topological spin texture, such as optical skyrmions, has attracted attention for applications such as excitation of in-solid-state skyrmions [8]. The exploration and realization of various topological spin textures in light is expected to lead to further understanding and applications of light and topology.

Recently, topological spin textures of light, called merons and antimerons, have been reported numerically in the band structure of valley photonic crystals (VPhCs) [9]. In this report, a honeycomb lattice PhC consisting of SiC slabs is used, as shown in Figure 1(a). By making the sublattice of the honeycomb lattice inequivalent, the degeneracy of the Dirac point at the K point is broken and a valley-shaped photonic band is formed. It has been reported that the band structure near the formed valley has a characteristic polarization distribution and forms meron and antimeron topological spin textures as shown in Figure 1 (b). In particular, the Dirac point on the upper side of the light line makes it possible to observe the band with optical input and output from outside the slab plane. For experiments, a method is proposed to calculate the polarization state in the band as a distribution of Stokes vectors by observing the polarization state of the band at each frequency as shown in Figure 1(c) and calculating the distribution of Stokes parameters as shown in Figure 1(d).

However, experimental observation of the spin texture requires design and fabrication of semiconductor nanostructures and advanced optical experiments for band structure

observation, which has not yet been reported. In addition, it is not clear whether the above Dirac point exists on the upper side of the light line because the refractive index of Si slab PhC, which is easy to fabricate, is higher than that of SiC. It is necessary to re-design the structure based on materials and parameters in line with experiments to find a structure that can be expected to be observed.

The purpose of this study is to experimentally observe the meron and antimeron optical spin textures in the band structure of VPhC. First, we will design and fabricate a structure suitable for the observation of the spin textures using Si slab PhC, for which fabrication techniques have been established. Next, we will measure the band structure of the VPhC using a microscope developed for photonic band structure measurements [10]. In particular, we will perform polarization-resolved band measurements to reveal the optical spin texture in the band structure and to experimentally observe merons and antimerons.

## Results and Discussion

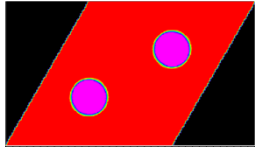
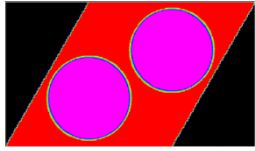
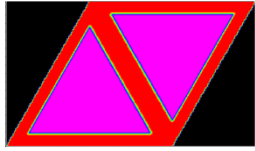
### (1) Design of VPhCs

While previous studies used a structure that assumes a SiC slab PhC, this study employs a Si slab PhC with a thickness of 220 nm, a fabrication technique that is mature in our group. Since the material and thickness of the PhC are different from those in the previous study, we designed the PhC for experimental observation. The parameters of the considered PhC structure are shown in Table 1 and its photonic band diagram is shown in Figure 2. The band structure was calculated using the three-dimensional plane wave expansion method.

Table 1(a) shows the structural parameters presented in the previous study [9] applied to a 220 nm thick Si slab PhC, which has a honeycomb lattice of circular air holes with a diameter of  $0.22a$ . Figure 2(a) shows its photonic band structure, and it can be seen that the Dirac point, which was previously focused on, comes below the light line due to the higher refractive index of the slab compared to previous studies. Under these conditions, the band cannot be observed by light irradiation from outside the slab surface and is not suitable for the present observation.

To increase the frequency of the band, the air holes must be enlarged to reduce the effective refractive index. The structure with larger diameter circular air holes is shown in Table 1(b) and its band diagram is shown in Figure 2(b). Compared to Figure 2(a), the frequency of the Dirac point is higher, indicating that it moves to almost the same frequency as the light line. On the other hand, in this experiment, since the light is input and output from outside the slab surface using an objective lens, the frequency of the band that can be observed depends on the NA of the objective lens. In general,  $NA < 1$  ( $NA = 0.9$  in this study), so the frequency

Table 1 PhC structures considered. (a) The PhC in the previous study is replaced by Si and the thickness is changed to 220 nm. (b) Structure from (a) with the size of the circular air pore enlarged. (c) The shape of the air pore is changed to triangular.

Structure	(a)	(b)	(c)
Material	Si	Si	Si
Refractive index	3.48	3.48	3.48
Lattice	Honeycomb	Honeycomb	Honeycomb
Period $a$	1200 nm	1200 nm	1200 nm
Slab thickness	220 nm	220 nm	220 nm
Shape of the air hole	Circle	Circle	Triangle
Diameter/Side length	$0.22a$	$0.50a$	$1.4a/\sqrt{3}$
Unit cell			

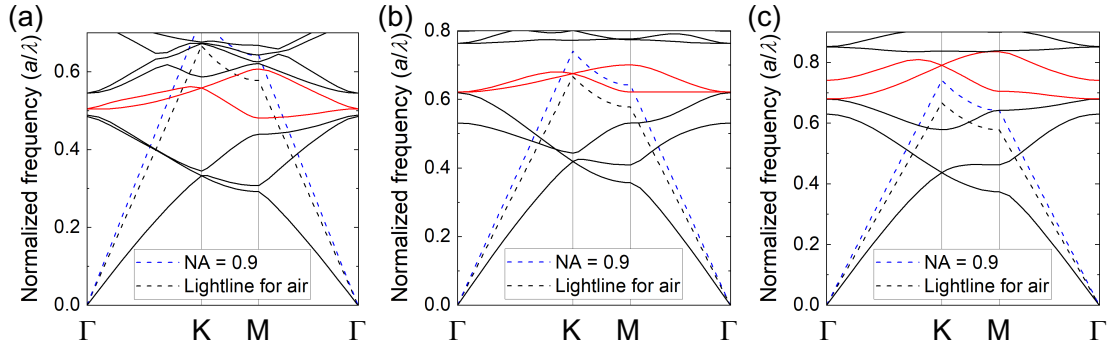


Fig. 2 Band diagram of the studied PhC structure. The red curve is the band with the Dirac-type dispersion relation we are focusing on. The black curves indicate other bands. The black dashed line is the light line at the air interface. The blue dashed line indicates the lower edge of the region focused by the objective lens with NA=0.9.

that can be observed is even higher than the light line. The frequency of the band in Fig. 2(b) is not suitable for the present design because it is outside the range (above the blue dashed line) that can be focused by an objective lens with NA=0.9.

To further increase the frequency of the Dirac point, the percentage of air holes in the PhC must be further increased. However, if the diameter of the circular air holes is further increased, the air holes become connected to each other, making fabrication difficult.

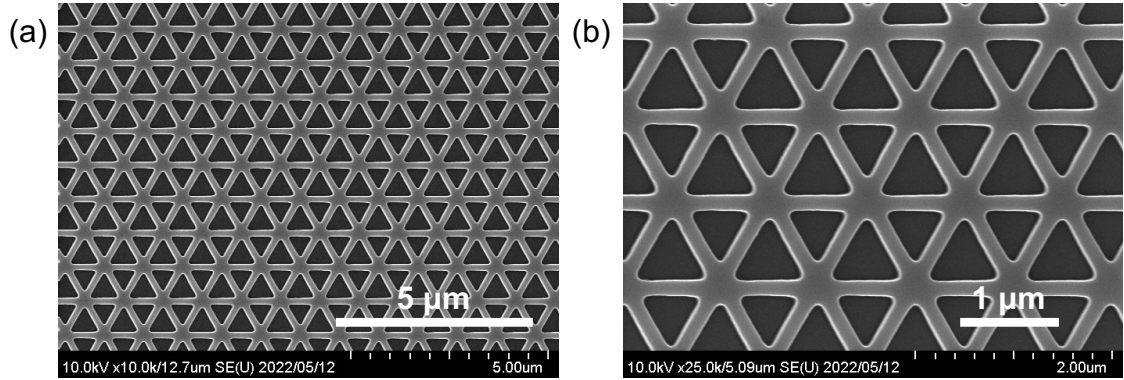


Fig. 3 (a) Scanning microscope image of the fabricated VPhC. (b) Enlarged image.

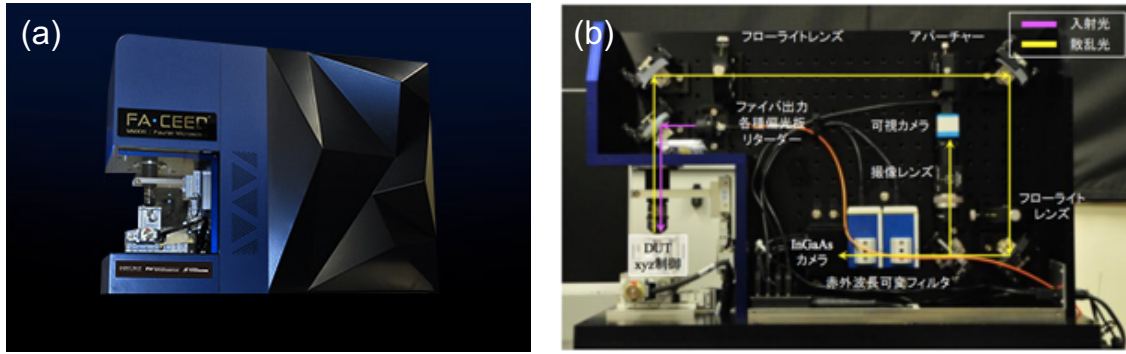


Fig. 4 Photonic band microscope. (a) Appearance. (b) Structure. [10]

Therefore, in this study, a honeycomb lattice with triangular-shaped air holes was adopted to increase the ratio of air holes. The structure is shown in Table 1(c) and the band diagram is shown in Figure 2(c). It can be seen that the Dirac point is located on the upper side of the light line due to the further increase in the percentage of air holes.

From the above discussion, it can be seen that a design based on structure (c) is desirable for the observation of spin texture using a Si slab VPhC with a thickness of 220 nm. For the observation, we will use a structure that breaks the degeneracy of the Dirac point by making the sizes of the two air holes of the sublattice inequivalent further from structure (c). In the following experiments, we used the structure with the lattice constant of  $a = 1000$  nm and side lengths of the triangular air hole as  $1.3a/\sqrt{3}$  and  $1.1a/\sqrt{3}$ .

## (2) Fabrication of VPhCs

Si slab VPhC was fabricated based on the design in (1), and a semiconductor nanofabrication

process using electron beam lithography and reactive ion etching was performed on the SOI substrate. Scanning electron microscope images of the fabricated VPhC are shown in Figure 3. It can be seen that a honeycomb lattice PhC with triangular air holes of two different sizes was fabricated as designed.

In section (1), an air-bridged PhC was used for ease of analysis, but in the experiment, an SiO<sub>2</sub> BOX layer was remained in the structure. This is because it is necessary to prepare a PhC of about 100 μm square for observation with a photonic band structure microscope, and an extra process is required to fabricate a large-area air-bridged PhC.

### (3) Polarization resolved photonic band measurements

For the measurement of the photonic band structure, we used a photonic band structure microscope [10] developed at Nishiyama Laboratory of the Tokyo Institute of Technology. Figure 4 shows an overview of the system. After the sample is set on the stage, it is illuminated by light from a white light source through an objective lens; after coupling to the state in PhC, the emitted light passes through the objective lens again and is cut out by a wavelength tunable filter, after which the far-field distribution is imaged by a near-infrared InGaAs camera. By scanning the wavelength of the filter, it is possible to observe the band structure in the band 950 – 1700 nm.

In this study, since it is necessary to observe the polarization distribution, polarization elements were introduced into the microscope to perform polarization-resolved photonic band measurements. Three polarization elements, a quarter-wave plate (QWP), a half-wave plate (HWP), and a linear polarizer (LP), were used. By measuring a total of four different band diagrams at different angles, the polarization state (Stokes parameters  $S_0 \sim S_3$ , see Appendix) of each point on the band was identified.

### (4) Analysis of polarization distributions

Figure 5 shows the polarization distributions in momentum space at 1211 nm wavelength. (a) – (d) correspond to  $S_0$ ,  $S_1/\sqrt{S_1^2 + S_2^2 + S_3^2}$ ,  $S_2/\sqrt{S_1^2 + S_2^2 + S_3^2}$ , and  $S_3/\sqrt{S_1^2 + S_2^2 + S_3^2}$ , respectively. (b) – (d) are normalized by  $\sqrt{S_1^2 + S_2^2 + S_3^2}$  because the degree of polarization is not unity. In the  $S_3$  distribution shown in Fig. 5(d), it can be seen that circularly polarized light with opposite directions in the K and K' directions are alternately aligned (the area circled by the white ellipses). This result is consistent with the trend of the VPhC polarization distribution and suggests the presence of meron or antimeron spin texture.

Figure 6 shows the polarization distribution in momentum space at a wavelength of 1293 nm.

In the  $S_0$  distribution shown in Fig. 6(a), a triangular shape of the intensity can be seen in the K and K' directions. This is consistent with the shape of the cross section of the valley section cut in the isofrequency plane, and it can be inferred that the band structure around the valley can be observed. Furthermore, in Fig. 6(b) and (c), the characteristic distributions seen in meron and antimeron spin textures can be confirmed (the area indicated by the white circle), indicating the presence of the spin texture.

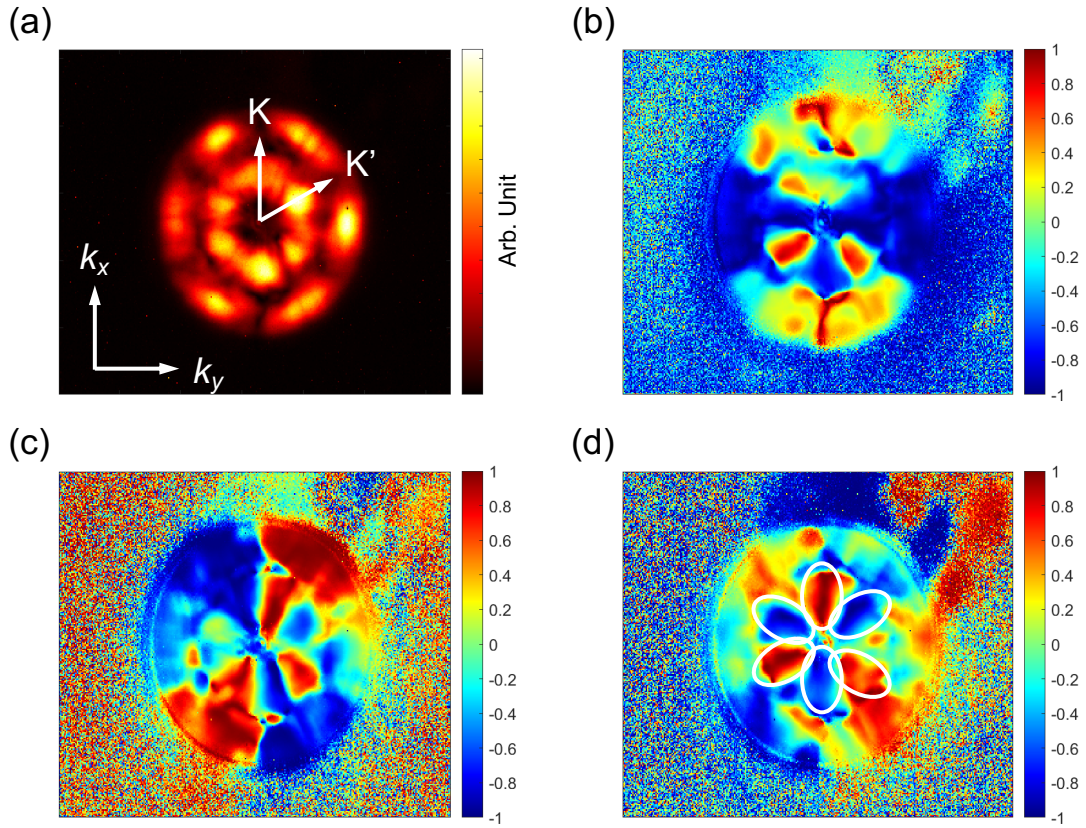


Fig. 5 Polarization distributions in momentum space at 1211 nm.

(a)  $S_0$ , (b)  $S_1/\sqrt{S_1^2 + S_2^2 + S_3^2}$ , (c)  $S_2/\sqrt{S_1^2 + S_2^2 + S_3^2}$ , and (d)  $S_3/\sqrt{S_1^2 + S_2^2 + S_3^2}$ .



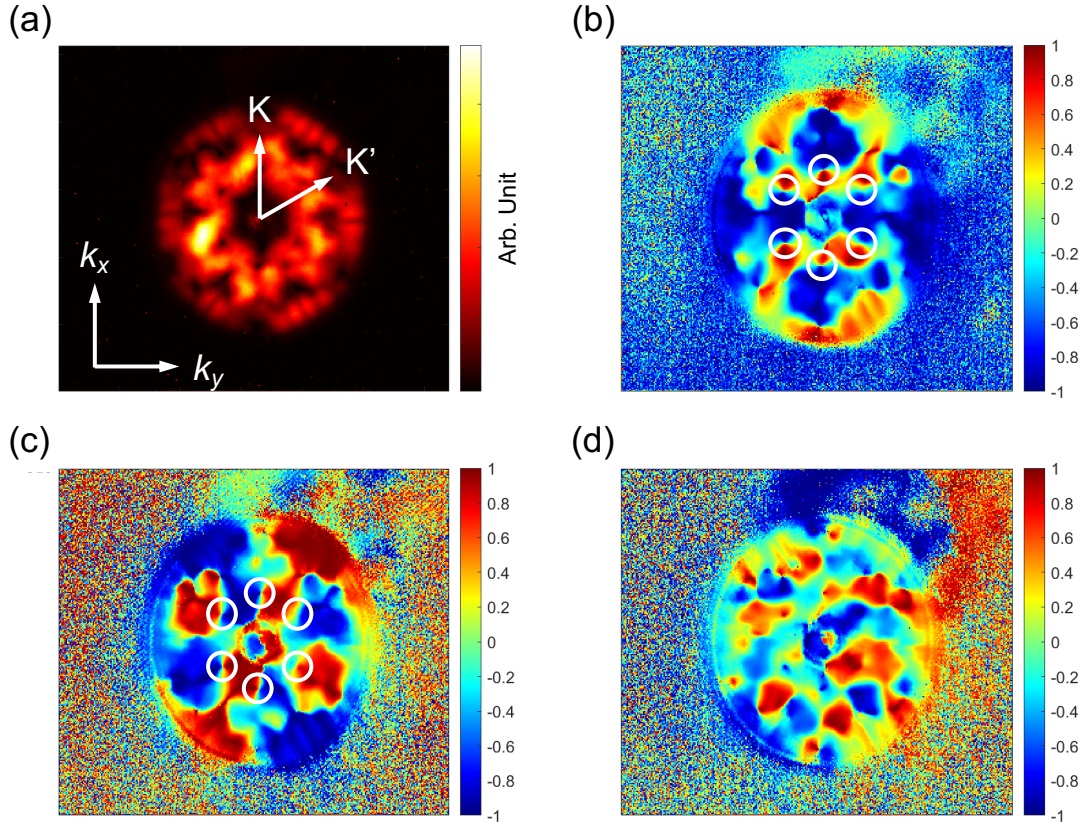


Fig. 6 Polarization distributions in momentum space at 1293 nm.

(a)  $S_0$ , (b)  $S_1/\sqrt{S_1^2 + S_2^2 + S_3^2}$ , (c)  $S_2/\sqrt{S_1^2 + S_2^2 + S_3^2}$ , and (d)  $S_3/\sqrt{S_1^2 + S_2^2 + S_3^2}$ .

## Conclusion and future prospect

In this research, we worked on the observation of meron and antimeron spin textures in the band structure of VPhC, designed and fabricated devices, and performed polarization-resolved band measurements. The VPhC was designed based on this structure. The band structure of the fabricated VPhC was measured by photonic band structure microscopy, and the polarization distribution in momentum space was calculated. As a result, we found the polarization distribution that suggests the existence of meron and antimeron.

Further analysis will be performed to demonstrate the observation of melon and antimeron spin texture.

## Appendix

Stokes parameters



Stokes parameters are a method of expressing the polarization state of light. They are composed of four real numbers  $S_0 - S_3$ , and are expressed by using the complex amplitudes of the electric field  $E_x$  and  $E_y$ .

$$\begin{aligned}S_0 &= |E_x|^2 + |E_y|^2 \\S_1 &= |E_x|^2 - |E_y|^2 \\S_2 &= 2\text{Re}E_x^*E_y \\S_3 &= 2\text{Im}E_x^*E_y\end{aligned}$$

$S_0$  means the intensity of light. For the completely polarized light,  $S_0^2 = S_1^2 + S_2^2 + S_3^2$ , and for the completely unpolarized light,  $S_1 = S_2 = S_3 = 0$ .  $S_1 = \pm 1$  correspond to the linear polarizations in vertical and horizontal directions,  $S_2 = \pm 1$  correspond to the inclined linear polarizations in  $\pm 45$  deg., and  $S_3 = \pm 1$  correspond to the right and left circular polarizations. Please see the textbooks on optics in detail [11].

## Acknowledgement

We would like to thank our supervisors, Prof. Iwamoto and Prof. Nishiyama, for their great support and guidance in carrying out this research. We would like to express our deepest gratitude to them. We are also deeply grateful to the secondary advisor, Prof. Kondo, for his useful advice.

## References

- [1] T. Ozawa *et al.*, Rev. Mod. Phys. **91**, 015006 (2019).
- [2] Z. Wang *et al.*, Nature **461**, 772 (2009).
- [3] M. I. Shalaev *et al.*, Nat. Nanotechnol. **14**, 31 (2019).
- [4] B. Bahari *et al.*, Science **358**, 636 (2017).
- [5] L. -G. Wang, Opt. Express **20**, 20814 (2012).
- [6] G. Milione *et al.*, Opt. Lett. **40**, 4887 (2015).
- [7] M. Kraus *et al.*, Opt. Express **18**, 22305 (2010).
- [8] S. Donati *et al.*, Proc. Natl. Acad. Sci. USA **113**, 14926 (2016).
- [9] C. Guo *et al.*, Phys. Rev. Lett. **124**, 106103 (2020).
- [10] T. Amemiya *et al.*, Opt. Lett. **47**, 2430 (2022).
- [11] E. Hecht, Pearson Education Limited *Fifth Edition* (2016).